

Dual Printed Antenna for Wi-Fi Applications

Ernesto Ávila-Navarro, José A. Carrasco, and Candid Reig, *Senior Member, IEEE*

Abstract—A dual-frequency compact printed antenna for Wi-Fi (IEEE 802.11x at 2.45 and 5.5 GHz) applications is presented. The design is successfully optimized using a finite-difference time-domain (FDTD)-algorithm-based procedure. Some prototypes have been fabricated and measured, displaying a very good performance.

Index Terms—Dipole antennas, dual-band antennas, printed antennas, Wi-Fi antennas.

I. INTRODUCTION

AMONG the several current wireless communication standards, Wi-Fi is nowadays rapidly gaining more and more supporters. The Wi-Fi standard is based on the well-established protocols IEEE 802.11a, 802.11b, 802.11g, and the emerging 802.11n. The considered operating frequencies are in the industrial, scientific, and medical (ISM) free window. More specifically, the 802.11b and 802.11g protocols make use of the band between 2.412 and 2.484 GHz (2.45-GHz center frequency and 72-MHz bandwidth), the 802.11a makes use of the band between 5.170 and 5.805 GHz (5.5-GHz center frequency and 635-MHz bandwidth), and the 802.11n protocol makes use of both frequency bands simultaneously. Devices designed to operate under these protocols require the use of compact dual-frequency antennas matching these specifications [1]. The use of printed technologies in these cases is almost mandatory [2], [3].

In this letter, we introduce a novel Yagi-like, printed-dipole dual antenna for Wi-Fi applications in the dual band 2.45/5.5 GHz. The antenna has been modeled and analyzed by means of an own code based on the finite-difference time-domain (FDTD) algorithm. The antenna has been fabricated and characterized with the help of an E8363B network analyzer and an anechoic chamber.

II. ANTENNA DESIGN

The proposed antenna is based on the resonant properties of grouped printed dipoles. A scheme is shown in Fig. 1. The considered substrate is clad ($\epsilon_r = 3.2$; $h = 1.52$ mm). Both groups of dipoles are designed to operate in a different frequency band. For proper radiation functionality, shorter dipoles are arranged to be closer to the feed point.

For each group, the number of dipoles and the scaling factor (τ) must be defined. Even though both parameters can be different from one group to another, we will use the same values

Manuscript received April 08, 2009; revised May 04, 2009. First published May 26, 2009; current version published July 01, 2009.

E. Ávila-Navarro and J. A. Carrasco are with the Departamento de Ciencia de Materiales, Óptica y Tecnología Electrónica, Universidad Miguel Hernández, Elche 03202, Spain.

C. Reig is with the Department of Electronic Engineering, Universitat de València, Burjassot 46100, Spain (e-mail: candid.reig@uv.es).

Color versions of one or more of the figures in this letter are available online at <http://ieeexplore.ieee.org>.

Digital Object Identifier 10.1109/LAWP.2009.2023542

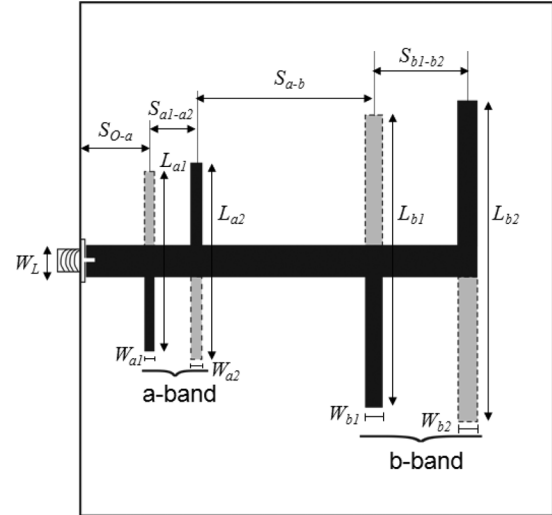


Fig. 1. Antenna scheme.

for both groups. The number of dipoles of each group is conditioned by the bandwidth and gain requirements of the specific band. Both bandwidth and gain increase with the increasing of the number of dipoles. Due to the moderate bandwidth requirements of the bands, and as will be demonstrated later, two dipoles per group are enough. The scale factor is defined as follows:

$$\tau = \frac{L_{g1}}{L_{g2}} = \frac{S_{g1}}{S_{g2}} = \frac{W_{g1}}{W_{g2}}$$

as defined for traditional log-periodic antennas [4], and substituting g by a or b , respectively. The symbols are detailed in Fig. 1. Typical values for τ range from 0.7 to 0.95. A widely accepted tradeoff is $\tau = 0.88$ [4]. We have considered the same scaling factor for both dipole groups.

Due to the configuration of the dipoles (each arm onto opposite faces of the substrate), the electrical length of the dipoles highly depends on the substrate characteristics (mainly the dielectric constant) and the considered frequency. The exact length of the dipoles is calculated through specific simulations. We used a FDTD-based code, initially designed for radar applications [5] and recently readapted to printed antennas analysis [4], [6]. Therefore, obtained lengths lie in the range $0.3\lambda_0$ – $0.4\lambda_0$, quite lower than the common $0.5\lambda_0$. To get a $50\text{-}\Omega$ input impedance, we selected $W_L = 3$ mm for input strip, as well as for the biggest dipole. The other widths are obtained by applying the scaling factor.

Parameter S_{0-a} needs to be longer enough in order to allow a good wave conformation. A value of $\lambda_g/2$ (for the highest operation frequency) has been demonstrated to be optimal [4], [6]. The separation between dipoles within the same group is

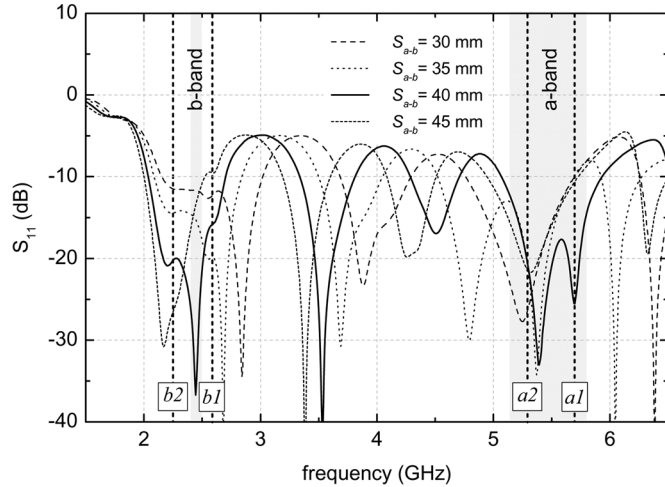

 Fig. 2. Simulation results as a function of S_{a-b} (defined in Fig. 1).

 TABLE I
 ANTENNA DIMENSIONS

| a-band (5.5 GHz) – $\tau=0.88$ | | | | |
|---------------------------------|----------|-------------------|------------------|----------------------|
| Dip. | Freq. | Length | Width | Separation |
| $a1$ | 5.9 GHz | $L_{a1}=19.29$ mm | $W_{a1}=1.76$ mm | $S_{0-a}=15.88$ mm |
| $a2$ | 5.2 GHz | $L_{a2}=21.92$ mm | $W_{a2}=2.00$ mm | $S_{a1-a2}=9.29$ mm |
| b-band (2.45 GHz) – $\tau=0.88$ | | | | |
| Dip. | Freq. | Length | Width | Separation |
| $b1$ | 2.67 GHz | $L_{b1}=42.69$ mm | $W_{b1}=2.64$ mm | $S_{b1-b2}=20.76$ mm |
| $b2$ | 2.35 GHz | $L_{b2}=48.51$ mm | $W_{b2}=3.00$ mm | |
| $S_{a-b}=40.0$ mm | | | | |

obtained by using the following relationship, traditionally used in the design of log-periodic antennas [4]:

$$S_{g2-g1} = 2 \left(\frac{\lambda_{g2}}{2} - \frac{\lambda_{g1}}{2} \right) \frac{0.243\tau - 0.051}{1 - \tau}$$

with λ_{g1} and λ_{g2} being the wavelength in free-space at the resonant frequency of each dipole within the same group ($g = a$ or $g = b$).

Finally, in order to obtain S_{a-b} , we performed simulations ranging from 25 to 50 mm. A summary of the results is displayed in Fig. 2. As easily observed, the electrical behavior of the antenna is highly conditioned by this parameter. More specifically, we can differentiate between peaks related to the dipole resonances, labeled in the figure, and other higher order modes resonances. As expected, the former have a lower dependence with S_{a-b} , and the latter, associated to longitudinal resonances, strongly depend on it. As a tradeoff, the best S_{11} results were considered for $S_{a-b} \cong 40$ mm. With all, final dimensions of the antenna are summarized in Table I.

III. RESULTS

The antenna was then patterned and fabricated onto a clad substrate making use of the dimensions in Table I. Fig. 3 shows a photograph of the prototype (the rule is in centimeters).

Return losses were measured with a vectorial network analyzer. Fig. 4 displays both simulated and measured results. As

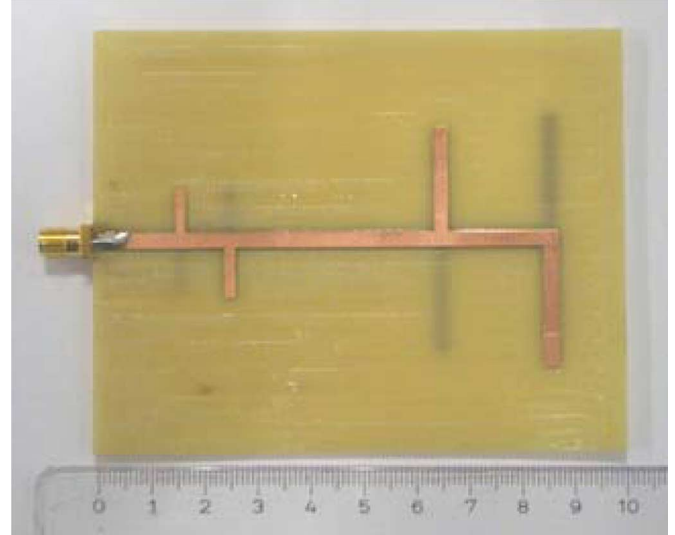


Fig. 3. Prototype photograph.

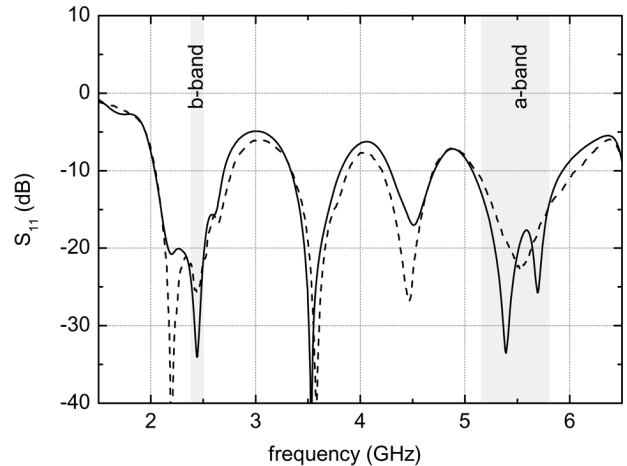


Fig. 4. Antenna return losses (— simulated, --- measured).

observed, there exists an excellent agreement between predictions and measurements along all the considered range. Additionally, we can appreciate an excellent matching between the S_{11} response and the band requirements, as also highlighted in Fig. 4.

For better understanding of the operation of the antenna, normalized electrical field y components, obtained by fast Fourier transform (FFT), are graphed in Fig. 5 for both operation frequencies. It is clearly observed how each group of dipoles is excited at the corresponding frequency.

Radiation patterns have also been calculated from near-to-far-field transformation and measured within an anechoic chamber for both planes and both operating band frequencies. The results are shown in Figs. 6 and 7, normalized to the maximum radiation level (180°). In both cases, we again observe the agreement between simulations and measurements, mainly for copolar components. A moderate directivity is also appreciated, due to the antenna configuration. At the high-band operation, low-band dipoles act as reflectors (see Fig. 5), increasing the gain in this band and forcing the backward radiation. Preferred applications of this antenna

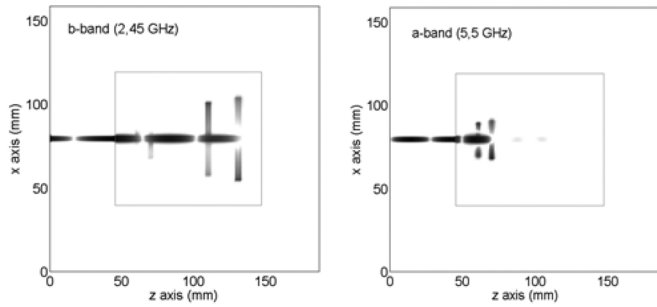


Fig. 5. Normalized electrical field distribution for both operation frequencies.

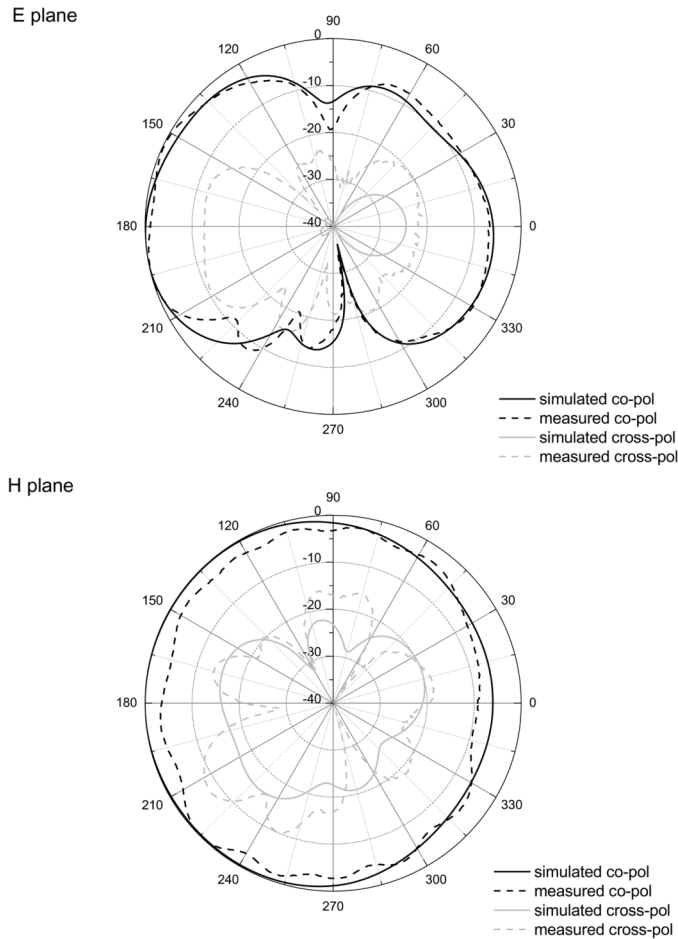


Fig. 6. Antenna radiation patterns at 2.45 GHz.

should be point-to-point links or parabolic antennas feeding more than handheld engines' built-in antennas. Finally, we also have measured and calculated the gain at both frequency bands: 2.2 dBi at 2.45 GHz (3 dBi when simulated) and 6.2 dBi at 5.5 GHz (6.5 dBi when simulated). This gain range is common in antennas for multiband applications (see, for example, [7]). The efficiency was also calculated giving values of 92% for 2.45 GHz and 94% for 5.5 GHz.

IV. CONCLUSION

A novel printed, dual-frequency antenna has been successfully developed for the Wi-Fi 2.45/5.5-GHz bands. Following a basic design together with an FDTD-based optimization proce-

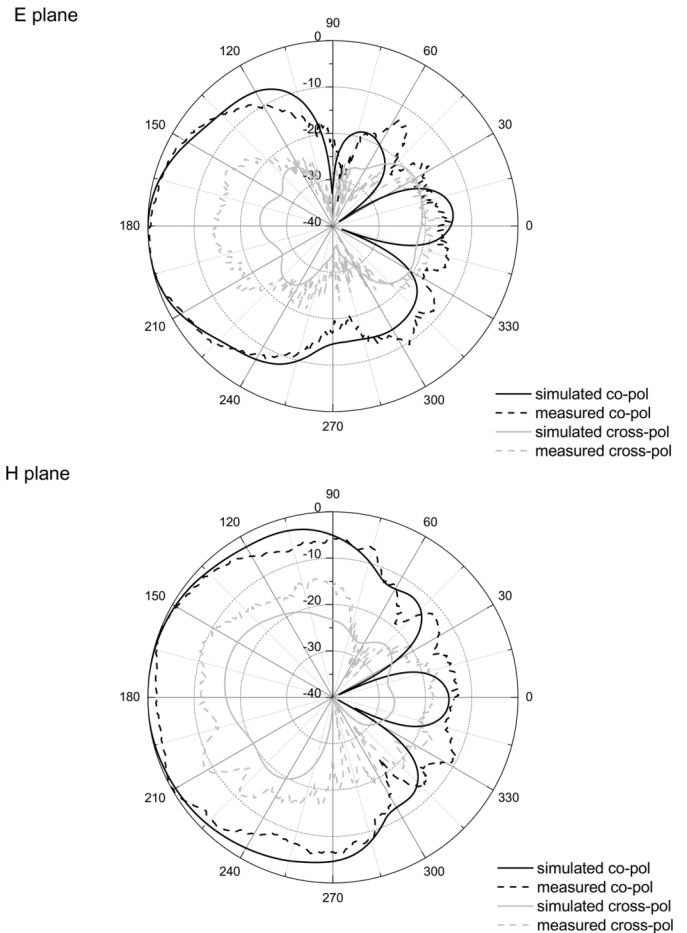


Fig. 7. Antenna radiation patterns at 5.5 GHz.

ture, the requirements of the considered bands, with regards to the bandwidth, can be suited. The radiation performance is adequate with gains varying from 2.2 to 6.2 dBi, depending on the working frequency.

ACKNOWLEDGMENT

The authors wish to thank J. P. Espinosa for his assistance with the antenna construction.

REFERENCES

- [1] P. Callaghan and J. C. Batchellor, "Dual-band pin-patch antenna for Wi-Fi applications," *IEEE Antennas Wireless Propag. Lett.*, vol. 7, pp. 757–760, 2008.
- [2] Y. J. Cho, Y. S. Shin, S. H. Hwang, and S.-O. Park, "A wideband internal antenna with dual monopole radiation elements," *IEEE Antennas Wireless Propag. Lett.*, vol. 4, pp. 381–384, 2005.
- [3] R. K. Joshi and A. R. Harish, "A modified bow-tie antenna for dual band applications," *IEEE Antennas Wireless Propag. Lett.*, vol. 6, pp. 468–471, 2007.
- [4] E. Ávila-Navarro, J. M. Blanes, J. A. Carrasco, and C. Reig, "A new bi-faced log periodic printed antenna," *Microw. Opt. Technol. Lett.*, vol. 48, pp. 402–405, 2006.
- [5] C. Reig, E. A. Navarro, and V. Such, "FDTD analysis of E-sectorial horn antennas for broad-band applications," *IEEE Trans. Antennas Propag.*, vol. 45, no. 10, pp. 1484–1487, Oct. 1997.
- [6] E. Ávila-Navarro, J. A. Carrasco, and C. Reig, "Design of Yagi-like printed antennas for WLAN applications," *Microw. Opt. Technol. Lett.*, vol. 49, pp. 2174–2178, 2007.
- [7] Y. Shin and S.-O. Park, "A compact loop type antenna for bluetooth, S-DMB, Wibro, WiMAX, and WLAN applications," *IEEE Antennas Wireless Propag. Lett.*, vol. 6, pp. 320–323, 2007.